



FULL LENGTH ARTICLE

PD_CD2 as a prognostic biomarker in glioma correlates with malignant phenotype



Fengsheng Dai ^{a,b,1}, Yixiao Yuan ^{a,1}, Jiaqi Hao ^{c,d,1},
Xing Cheng ^e, Xiangyi Zhou ^a, Li Zhou ^b, Rui Tian ^b, Yi Zhao ^b,
Tingxiu Xiang ^{a,b,*}

^a Department of Oncology, The First Affiliated Hospital of Chongqing Medical University, Chongqing 400010, China

^b Chongqing Key Laboratory of Translational Research for Cancer Metastasis and Individualized Treatment, Chongqing University Cancer Hospital, Chongqing 400030, China

^c Department of Neurosurgery, Xiangya Hospital, Central South University, Changsha, Hunan 410008, China

^d Hunan International Scientific and Technological Cooperation Base of Brain Tumor Research, Xiangya Hospital, Central South University, Changsha, Hunan 410008, China

^e Department of Neuro-Oncology, Chongqing University Cancer Hospital, Chongqing 400030, China

Received 28 March 2023; accepted 4 August 2023

Available online 21 September 2023

KEYWORDS

Biomarker;
Glioma;
Programmed cell death 2;
Progression;
Solid cancer

Abstract Programmed cell death 2 (PD_CD2) is related to cancer progression and chemotherapy sensitivity. The role of PD_CD2 in solid cancers (excluding hematopoietic malignancies) and their diagnosis and prognosis remains unclear. The TCGA, CGGA, GEPIA, cBioPortal, and GTEx databases were analyzed for expression, prognostic value, and genetic modifications of PD_CD2 in cancer patients. Functional enrichment analysis, CCK8, colony formation assay, transwell assay, and xenograft tumor model were undertaken to study the PD_CD2's biological function in glioma (GBMLGG). The PD_CD2 gene was associated with solid cancer progression. In the functional enrichment analysis results, PD_CD2 was shown to participate in several important GBMLGG biological processes. GBMLGG cells may be inhibited in their proliferation, migration, invasion, and xenograft tumor growth by knocking down PD_CD2. Our research can provide new insights into solid cancer prognostic biomarkers of PD_CD2.

© 2023 The Authors. Publishing services by Elsevier B.V. on behalf of KeAi Communications Co., Ltd. This is an open access article under the CC BY license (<http://creativecommons.org/licenses/by/4.0/>).

* Corresponding author. Department of Oncology, The First Affiliated Hospital of Chongqing Medical University, Chongqing 400010, China.
E-mail address: xiangtx@cqmu.edu.cn (T. Xiang).

Peer review under responsibility of Chongqing Medical University.

¹ These authors contributed equally to this work.

Introduction

Cancer is still a major disease threatening human health worldwide, bringing serious economic and medical burdens to society.¹ Despite improvements in cancer diagnosis and treatment in recent years, some patients still have poor prognosis.^{2,3} The discovery of potentially reliable and characteristic biomarkers for cancer diagnosis and treatment is therefore crucial for improving cancer patient survival and prognosis.

Programmed cell death 2 (PDCD2) was first detected in rats,⁴ and is essential for the development of mice and fruit flies during embryonic development.^{5,6} In human cells, PDCD2 could participate in ribosome assembly as a ribosomal chaperone protein.⁷ PDCD2 has been shown to be associated with B-cell malignant tumors and is regarded as a target gene of BCL6, and patients with acute leukemia can be monitored by PDCD2.^{8–10} Emerging evidence has indicated that PDCD2 acts as a tumor suppressor in gastrointestinal stromal tumors,¹¹ liver cancer,¹² and gastric cancer.¹³ A sufficient understanding of PDCD2's role in carcinogenesis is still lacking, however.

Here, we examined the expression level, clinical characteristics, prognostic value, and mutation status of PDCD2 in solid cancers. PDCD2 was also evaluated on glioma (GBMLGG) cells using the CCK8, colony formation, transwell assays, and xenograft tumor model. Our findings indicate that PDCD2 could be used for cancer diagnosis and prognosis and as a molecular target for GBMLGG.

Materials and methods

Data acquisition and processing

Data from The Cancer Genome Atlas (TCGA) website (<https://portal.gdc.cancer.gov/repository>) and the Genotype-Tissue Expression (GTEx) database were applied.¹⁴ Furthermore, we obtained clinical and sequencing information from more than 2000 brain tumor samples sourced from the Chinese Glioma Genome Atlas (CGGA) website (<http://www.cgga.org.cn/>).¹⁵ Before analysis, the transcript per kilobase (TPM) values were standardized. Using the pROC and the ggplot2 package in R, the diagnostic value of PDCD2 was evaluated.

UALCAN

Solid cancers PDCD2 protein expression levels were assessed using the UALCAN portal (<http://ualcan.path.uab.edu>),^{16,17} which is an interactive web resource.

The prognostic and clinical information of PDCD2 in pan-cancer

We used the GEPIA database (<http://gepia.cancer-pku.cn/>)¹⁸ and the PrognoScan database (<http://dna00.bio.kyutech.ac.jp/PrognoScan/index.html>)¹⁹ to examine the prognostic values of PDCD2 in solid cancers. A cut-off value of 50% was used to divide cohorts with high and low expression.

The CCDC50 gene mutation in pan-cancer

Through the cBioPortal (<https://www.cbioportal.org/>),²⁰ we analyzed the mutation information in human cancer (excluded hematopoietic malignancies) for the PDCD2 gene.

Curve analysis of receiver operating characteristics (ROC)

To assess the diagnostic value of screening signature genes, we utilized the pROC function from the R package to generate receiver operating characteristic (ROC) curves and calculate the area under the curve (AUC).

Gene set enrichment analysis

Gene set enrichment analysis (GSEA) software (version 3.0) was obtained from GSEA²¹ and samples were divided into high expression ($\geq 50\%$) and low expression ($< 50\%$) groups according to the PDCD2 expression level. The c2.cp.kegg.v7.4.symbols.gmt subcollection was downloaded from the Molecular Signatures Database²² (<http://www.gsea-msigdb.org/gsea/downloads.jsp>). The minimum gene set is 5, the maximum gene set is 5000, and a thousand resamples were used to evaluate the related pathways and molecular mechanisms; a false discovery rate (FDR) < 0.05 and a P value < 0.05 were considered statistically significant.

Analysis of the protein and gene interaction networks

GeneMANIA²³ (<http://www.genemania.org>) and STRING²⁴ (<https://string-db.org/>) were utilized to build a network of interactions between genes and proteins associated with PDCD2.

Cell lines and cell culture

U251 and U87 glioma cell lines were bought from the Chinese Academy of Sciences (Shanghai, China) with STR document, and cultured in DMEM media (Lonza, CC3170) supplemented with 10% fetal bovine serum (FBS) and 1% penicillin/streptomycin.

Small interfering RNA (siRNA)

The siRNAs for PDCD2 (si-PDCD2#1: 5'-UGGUAGUU-GAUUCCUAACUCGCA-3'; si-PDCD2#2: 5'-UAUAAUCUCU-GAGUAUCUUCCUUUC-3') were synthesized by ORIGENE. As a negative control, scrambled siRNA was synthesized. Lipofectamine 3000 (Invitrogen) was used for transfection.

Quantitative real-time PCR

The qRT-PCR assay was performed as previously described.²⁵ The primer sequences were as follows: PDCD2-F: 5'-ACT CAT ATG AGC CAC CTT CTG AG-3'; PDCD2-R: 5'-GTC TGA TGC TCC TTG CTG CAG-3'; β -actin-F: 5'-TCC TGT GGC ATC CAC GAA

ACT-3'; β-actin-R: 5'-GAA GCA TTT GCG GTG GAC GAT-3'. Expression quantification was obtained with the $2^{-\Delta\Delta CT}$ method.

Western blotting

Western blotting was performed as previously described.²⁶ The primary antibodies used included PDCD2 (Proteintech, 10725-1-AP) and β-actin (sc-47778, Santa Cruz). Using a chemiluminescence kit (Amersham Pharmacia Biotech, Piscataway, NJ), protein bands were detected. All the experiments were repeated thrice.

Cell proliferation, colony formation assay, and transwell assay

At 0, 24, 48, 72, and 96 h after cell seeding, absorbance (at 450 nm) in each well was determined with CCK8 kit (C0037, Beyotime).²⁷ For colony formation assays, seeded cells in 6-well plates (800 cells/well) were then cultured for 10 days. Transwell assays were performed as previously described.^{26,28} All the experiments were repeated thrice.

Xenograft model studies

Male BALB/c nude mice, aged 4 weeks, were obtained from GemPharmatech Technology (Jiangsu, China). Each mouse's left flank was injected with U87 cells at a concentration of 4×10^6 cells/mouse. Nine mice were injected with si-NC or siRNA (10 nmol in 0.1 mL of saline buffer per tumor nodule) every 2 days for a total of nine injections. After 10 days, the xenograft models were divided into three groups ($n = 3$) once the tumors reached a size of approximately 6 mm × 5 mm. On Day 34, the tumor-bearing mice were euthanized by cervical dislocation after being anesthetized with isoflurane. The xenograft tumors were then dissected, weighed, and photographed.

Immunohistochemistry

The technique of immunohistochemistry (IHC) was carried out following the methods described earlier.^{28,29} The xenograft sections of nude mice were treated with primary antibodies against PDCD2 (Proteintech, 10725-1-AP) and Ki67 (sc-23900, Santa Cruz) for overnight incubation at 4 °C. Subsequently, they were exposed to a secondary antibody.

Statistical analysis

T-tests were used to estimate PDCD2 expression in pan-cancer. Correlations between clinicopathological characteristics and PDCD2 expression were assessed using Chi-square tests, Fisher's exact tests, Kruskal-Wallis tests, and Wilcoxon's signed rank tests. Cox logistic regression models with univariate and multivariate analyses were used to uncover clinical factors that affected survival and PDCD2 expression. The survival time of patients with high or low PDCD2 expression was analyzed by Kaplan-Meier analysis. The symbols ns, *, **, and *** indicate $P > 0.05$, $P < 0.05$, $P < 0.01$, and $P < 0.001$, respectively.

Results

Analysis of PDCD2 expressed in solid cancers

First, analysis of the TIMER database was carried out to examine the PDCD2 expression level in human solid cancers. We found that PDCD2 expression was increased in bladder urothelial carcinoma (BLCA), stomach adenocarcinoma (STAD), cholangiocarcinoma (CHOL), colon adenocarcinoma (COAD), glioblastoma multiforme (GBM), rectum adenocarcinoma (READ), liver hepatocellular carcinoma (LIHC), lung adenocarcinoma (LUAD), esophageal carcinoma (ESCA), lung squamous cell carcinoma (LUSC), prostate adenocarcinoma (PRAD), breast invasive carcinoma (BRCA), and uterine corpus endometrial carcinoma (UCEC) tissues compared with adjacent normal tissues. In addition, low expression of PDCD2 in cancer was observed in kidney clear cell carcinoma (KIRC), kidney chromophobe (KICH), and thyroid carcinoma (THCA) (Fig. 1A).

Next, we combined the TCGA and GTEx database, and the results confirmed that PDCD2 expression was significantly higher in GBM, GBMLGG, brain lower grade glioma (LGG), UCEC, BRCA, LUAD, stomach and esophageal carcinoma (STES), COAD, PRAD, STAD, head and neck squamous cell carcinoma (HNSC), LUSC, LIHC, skin cutaneous melanoma (SKCM), THCA, rectum adenocarcinoma (READ), esophageal carcinoma (ESCA), ovarian serous cystadenocarcinoma (OV), pancreatic adenocarcinoma (PAAD), testicular germ cell tumors (TGCT), uterine carcinosarcoma (UCS), and CHOL than in paired adjacent normal tissues (Fig. 1B). In order to investigate the level of PDCD2 protein in human solid cancers, we used UALCAN database analysis and proved that PDCD2 was highly expressed in BRCA, UCEC, LUAD, and GBM (Fig. 1C).

Prognostic values of PDCD2 in solid cancers

Since PDCD2 expression was differently expressed in many types of cancer, the ability of prognostic values of PDCD2 in human cancer was explored. A higher level of PDCD2 expression was associated with lower overall survival (OS) for adrenocortical carcinoma (ACC), GBMLGG, LIHC, and Sarcoma (SARC) (Fig. 2A), poor disease-specific survival (DSS) in ACC, GBMLGG, and UCEC (Fig. 2B), and poor progression-free interval (PFI) in ACC, GBMLGG, HNSC, LIHC, OV, and UCEC (Fig. 2C).

PDCD2 could act as a potential biomarker in solid cancers

To investigate whether PDCD2 could act as a biomarker in solid cancers, the ROC curve analysis was conducted, and the results indicated that PDCD2 could be used as a high sensitivity and specificity biomarker (AUC > 0.75) for diagnosing digestive system tumors such as CHOL, COAD, STAD, PAAD, and READ (Fig. 3A), chest tumors including esophageal adenocarcinoma (ESAD), ESCA, and LUSC (Fig. 3B), nervous system tumor GBMLGG including GBM and LGG (Fig. 3C), and genitourinary system tumors including KICH, TGCT, and UCS (Fig. 3D).

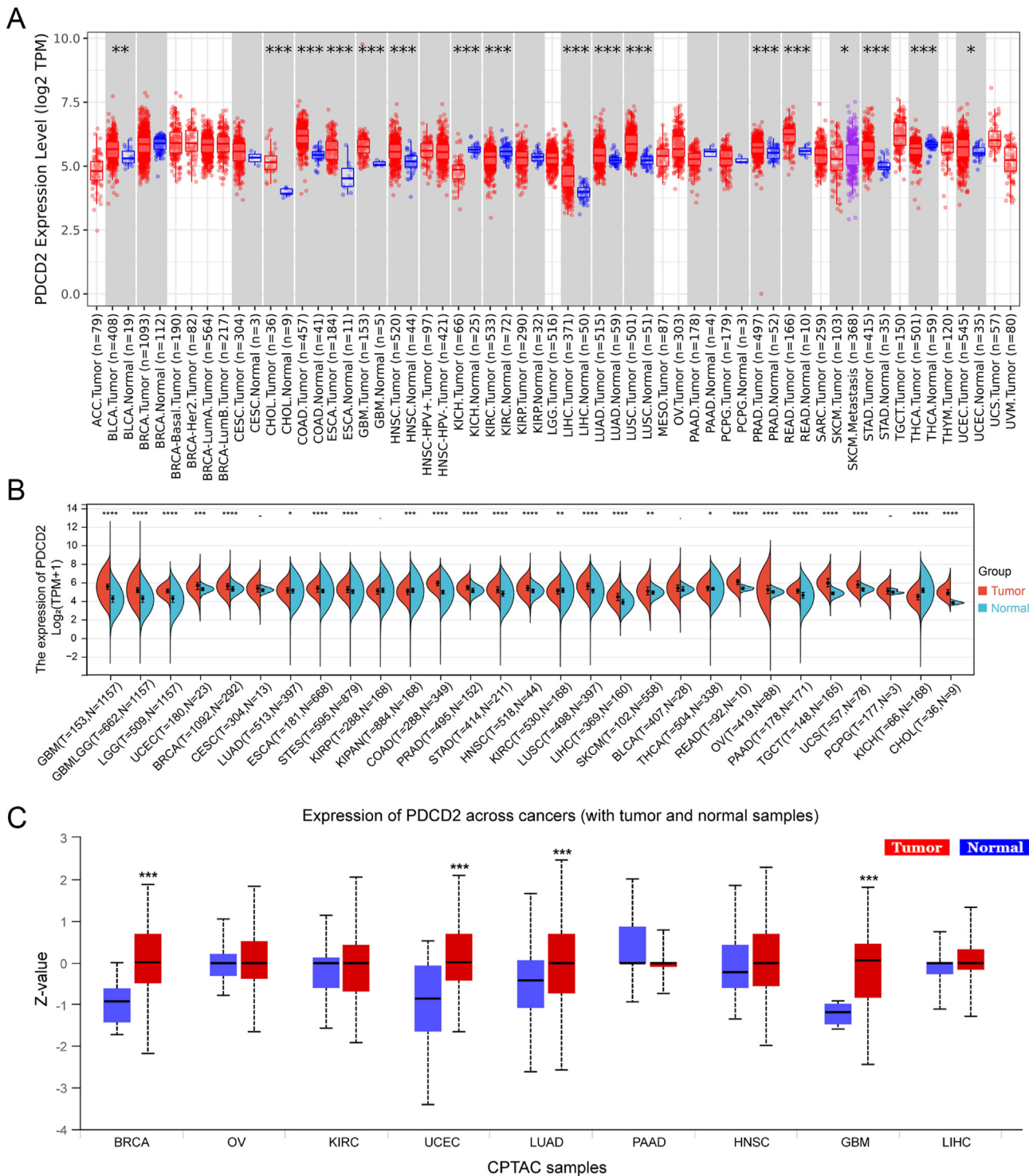


Figure 1 PDCD2 expression in pan-cancer. **(A)** Examining the TIMER database uncovers PDCD2 expression in pan-cancers. **(B)** Pan-cancer analysis of PDCD2 expression in TCGA/GTEX. **(C)** Data from the UALCAN database on PDCD2 protein in pan-cancer analysis. ns, $P > 0.05$; * $P < 0.05$, ** $P < 0.01$, *** $P < 0.001$.

Gene mutation landscape of PDCD2 in solid cancers

Data on PDCD2 mutations was downloaded from the cBio-Portal. To analyze the PDCD2 mutation landscape in human cancer, 33 missense sites, 4 truncation sites, and 1 fusion situated between amino acids 0 and 344 were identified in

PDCD2 ([Fig. 4A](#)). In addition, ocular melanoma, ACC, and the ovarian epithelial tumor had a higher mutation frequency than other cancers ([Fig. 4B](#)). Furthermore, we found that copy number variations (CNV) of PDCD2 regulate gene expression through different means (increasing or decreasing) in diverse cancer types ([Fig. 4C](#)). According to

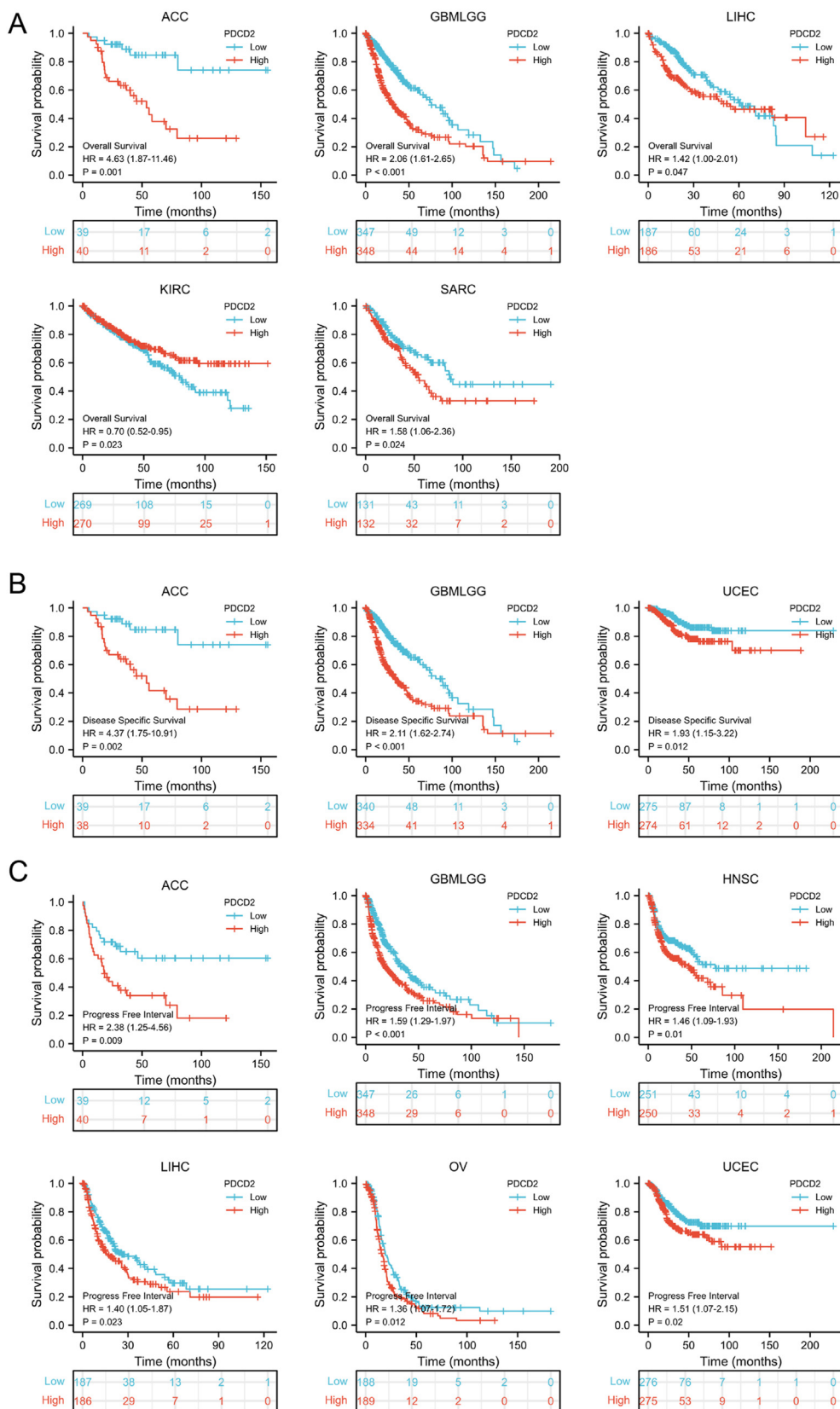


Figure 2 The PDCD2 prognostic values in pan-cancer. (A) The impact of PDCD2 expression on the overall survival rate of patients with ACC, GBMLGG, LIHC, KIRC, or SARC. (B) The disease-specific survival for PDCD2 in ACC, GBMLGG, and UCEC. (C) The progress-free survival for PDCD2 in ACC, GBMLGG, HNSC, LIHC, OV, and UCEC.

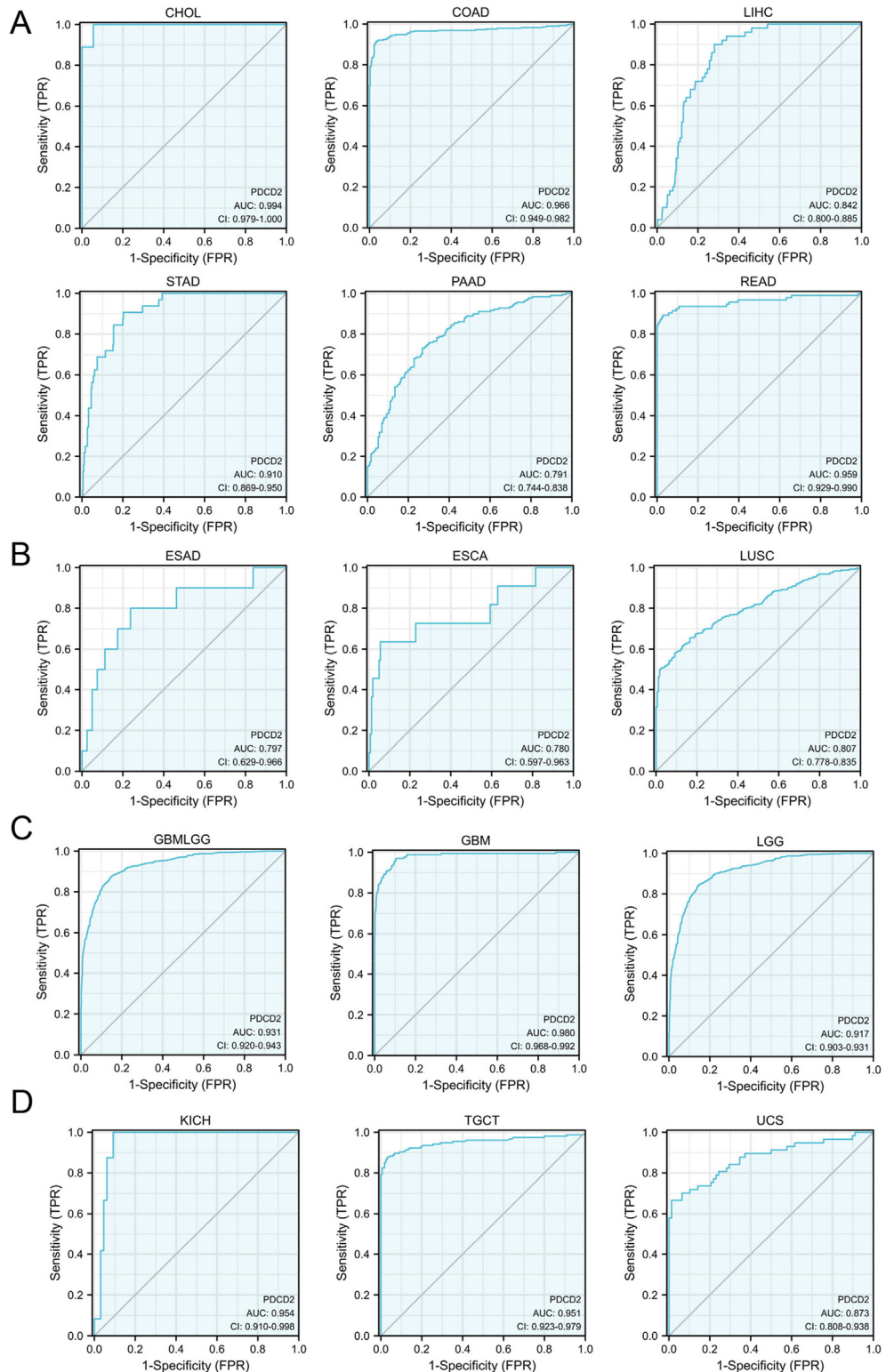


Figure 3 ROC curve analysis of PDCD2 in pan-cancer. ROC curve analysis of PDCD2 in CHOL, COAD, LIHC, STAD, PAAD, and READ (A), ESAD, ESCA, and LUSC (B), GBMLGG, GBM, and LGG (C), KICH, TGCT, and UCS (D). TPR, true positive rate; FPR, false positive rate.

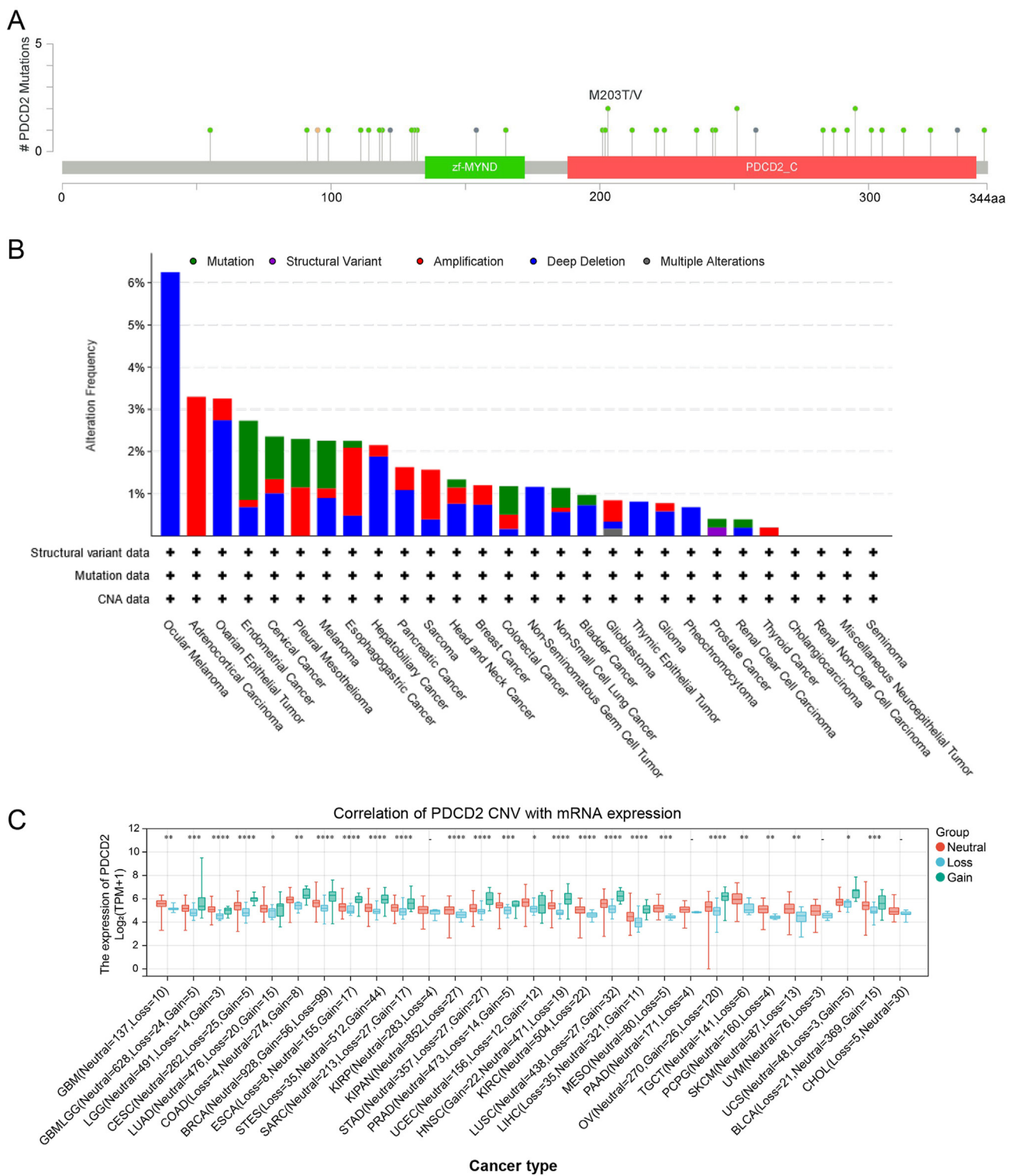


Figure 4 Mutational analysis of PDCD2. **(A)** Hot spots of mutation of PDCD2. **(B)** A summary of PDCD2 mutation types and their distribution among different cancers. **(C)** Correlation of PDCD2 CNV with mRNA expression in pan-cancer. ns, $P > 0.05$; * $P < 0.05$, ** $P < 0.01$, *** $P < 0.001$.

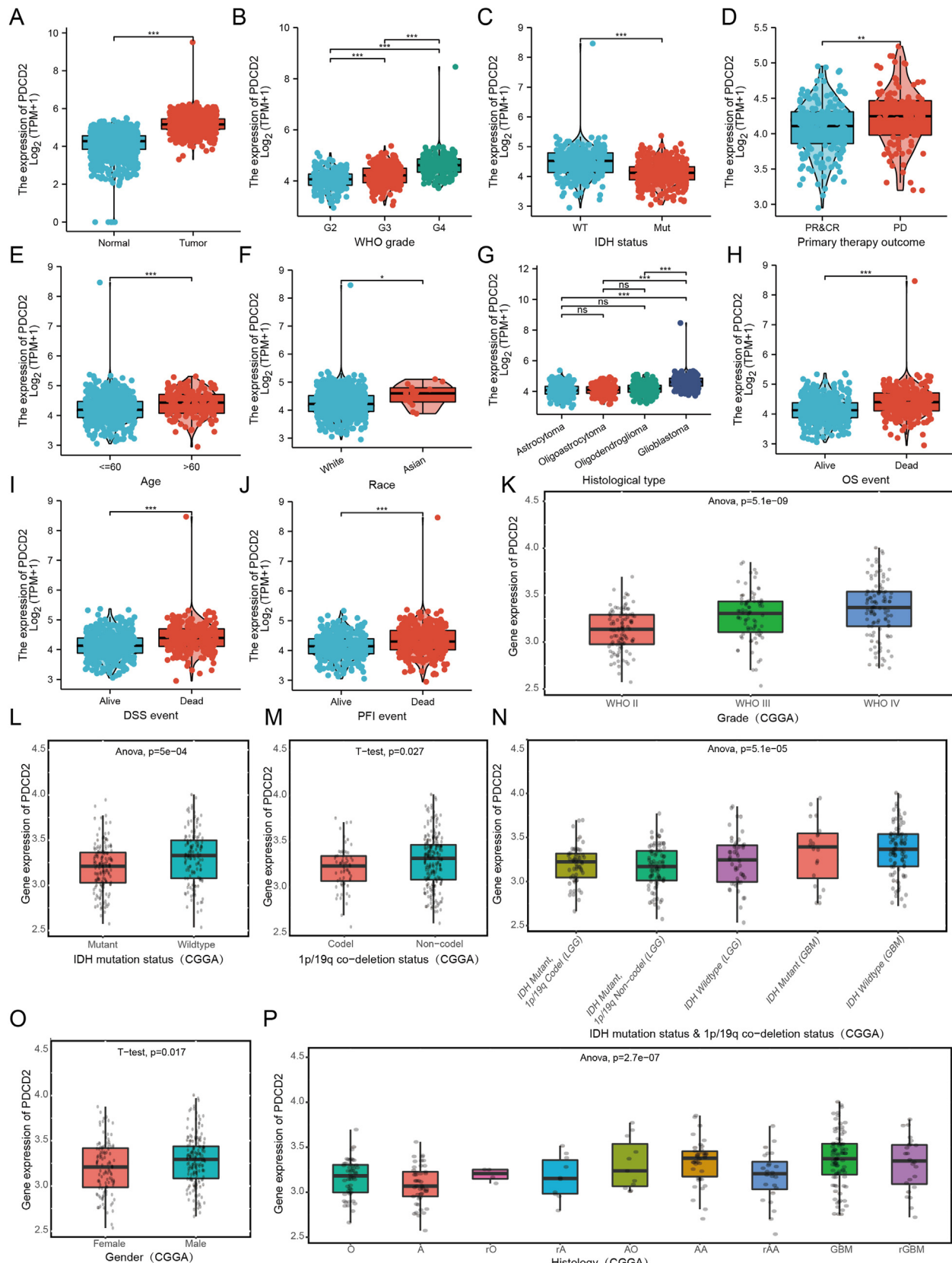


Figure 5 PDCD2 is correlated with clinical characteristics in GBMLGG (A), and associated with WHO grade, IDH status, primary therapy outcome, age, race, histological type, OS event, DSS event, and PFI event (B–J) (data from TCGA). PDCD2 is correlated with clinical characteristics in glioma, including the WHO grade, IDH mutation status, 1p/19q co-deletion status, IDH mutation status & 1p/19q co-deletion status, gender, and histology (K–P) (data from CGGA). G2,

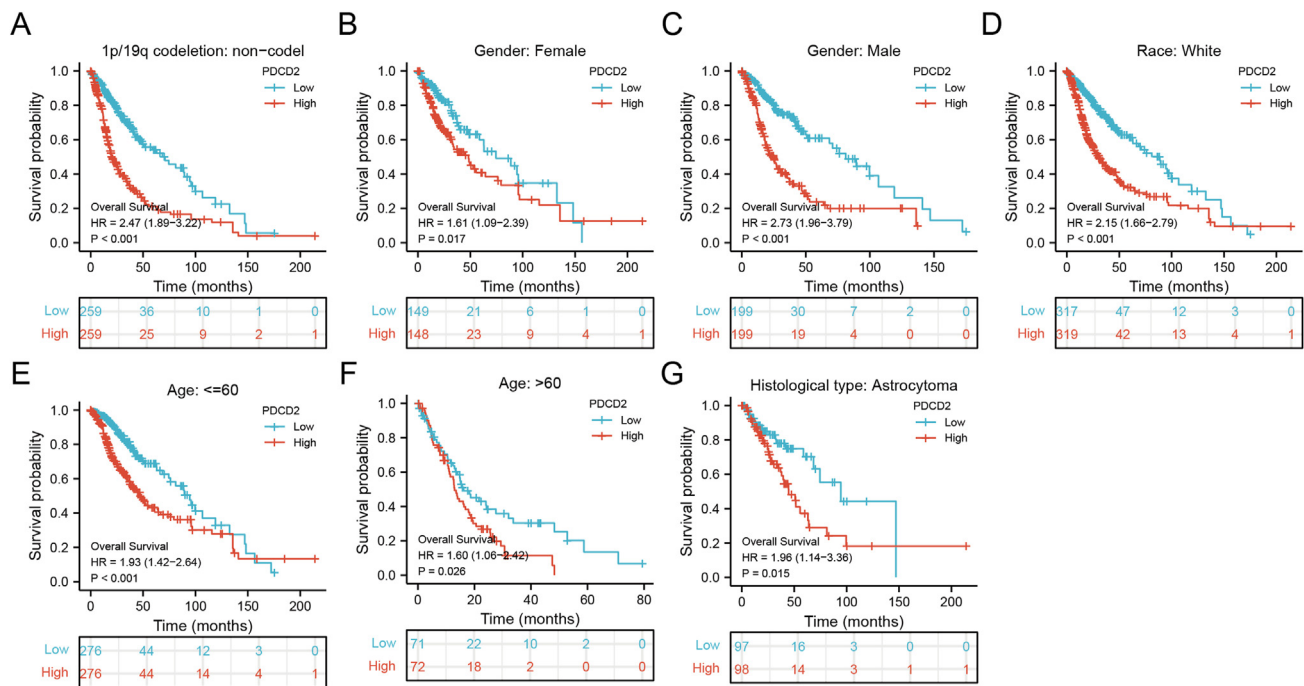


Figure 6 PDCD2 is correlated with prognosis in GBMLGG. The correlation between PDCD2 and OS in 1p/19q co-deletion status (A), gender (both female and male) (B, C), race (white) (D), age (E, F), and histological type (G) of GBMLGG.

Table 1 Univariate and multivariate Cox regression analyses of clinical characteristics associated with OS of glioma.

Characteristics	Total (N)	Univariate analysis		Multivariate analysis	
		Hazard ratio (95% CI)	P Value	Hazard ratio (95% CI)	P Value
WHO grade	634				
G2	223	Reference			
G3	243	2.999 (2.007–4.480)	< 0.001	2.638 (0.988–7.042)	0.053
G4	168	18.615 (12.460–27.812)	< 0.001	5.795 (1.142–29.396)	0.034
IDH status	685				
WT	246	Reference			
Mut	439	0.117 (0.090–0.152)	< 0.001	0.322 (0.144–0.721)	0.006
Primary therapy outcome	461				
PD	112	Reference			
SD	147	0.440 (0.294–0.658)	< 0.001	0.430 (0.180–1.025)	0.057
PR	64	0.170 (0.074–0.391)	< 0.001	0.272 (0.078–0.953)	0.042
CR	138	0.133 (0.064–0.278)	< 0.001	0.210 (0.069–0.634)	0.006
Age	695				
≤60	552	Reference			
>60	143	4.668 (3.598–6.056)	< 0.001	4.252 (1.924–9.397)	< 0.001
Histological type	363				
Astrocytoma	195	Reference			
Glioblastoma	168	6.160 (4.446–8.535)	< 0.001		
PDCD2	695	2.183 (1.840–2.590)	< 0.001	1.149 (0.615–2.147)	0.664

Bold value represents significant values.

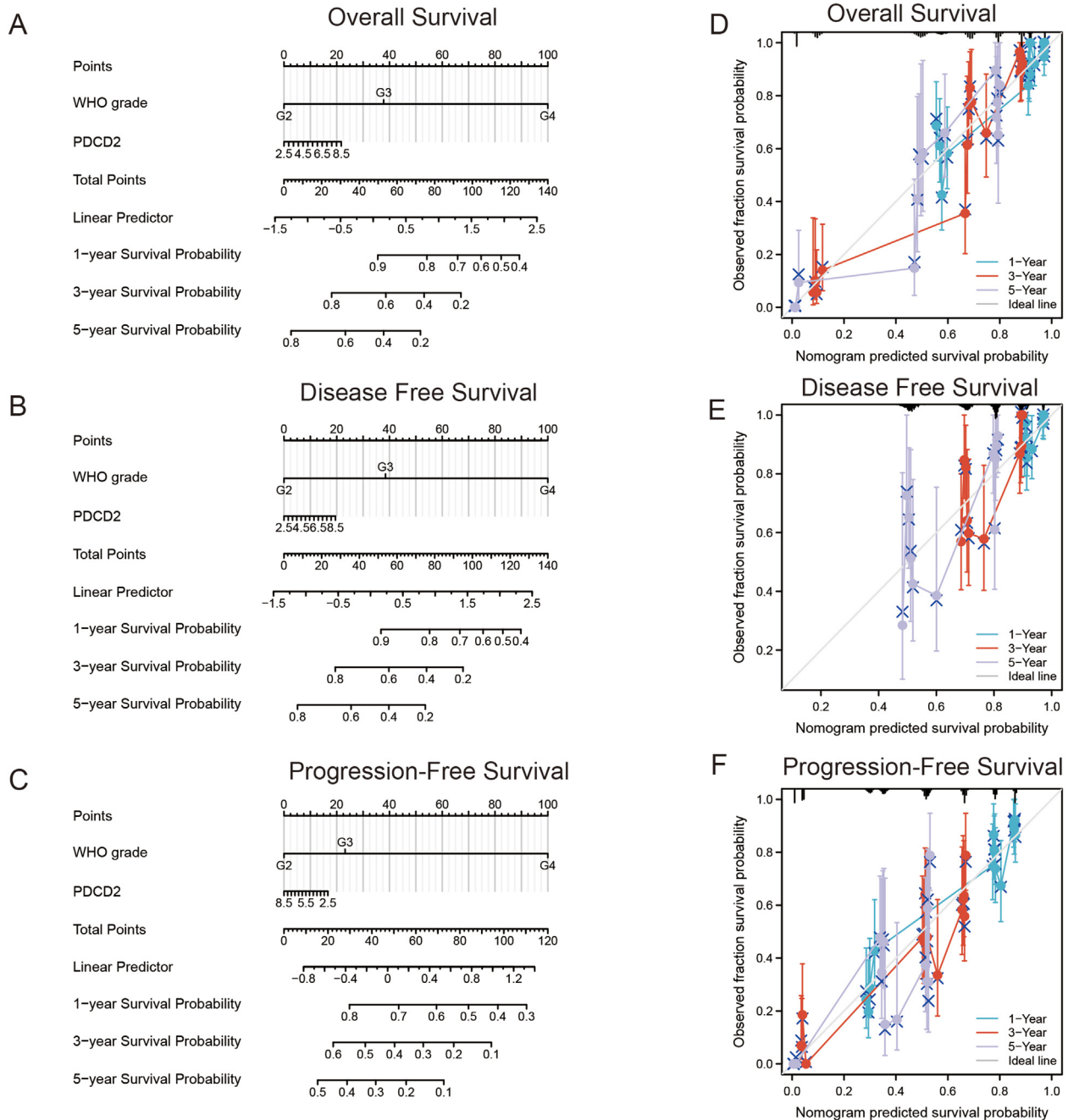


Figure 7 The ability of PDCD2 to predict the GBMLGG patients' prognosis. Construction and evaluation of nomogram used for predicting OS (A), DFS (B), and PFS (C) of GBMLGG patients. The calibration curve and Hosmer–Lemeshow test of nomograms in the TCGA-GBMLGG cohort for OS (D), DFS (E), and PFS (F).

these results, PDCD2 has different mutation forms in different tumor types.

PDCD2 as an independent prognostic factor for GBMLGG

It appears that PDCD2 plays an important biological role in GBMLGG. Next, we examined the relationship between PDCD2 expression and GBMLGG clinical features. Data from TCGA showed that high PDCD2 expression was strongly associated with WHO grade, IDH status, primary therapy

outcome, age, race, histological type, OS event, DSS event, and PFI event (Fig. 5A–G). Similarly, CGGA database¹⁵ indicated that high PDCD2 expression was significantly associated with 1p/19q co-deletion status, grade, IDH mutation status, gender, and IDH mutation status & 1p/19q co-deletion status (Fig. 5K–P). Using the Rembrandt database³⁰ and the Gravendeel database,³¹ an association between PDCD2 expression and GBMLGG grade and histology also was found (Fig. S1).

We continued to explore the prognostic analysis of GBMLGG patients and PDCD2 expression in TCGA. In

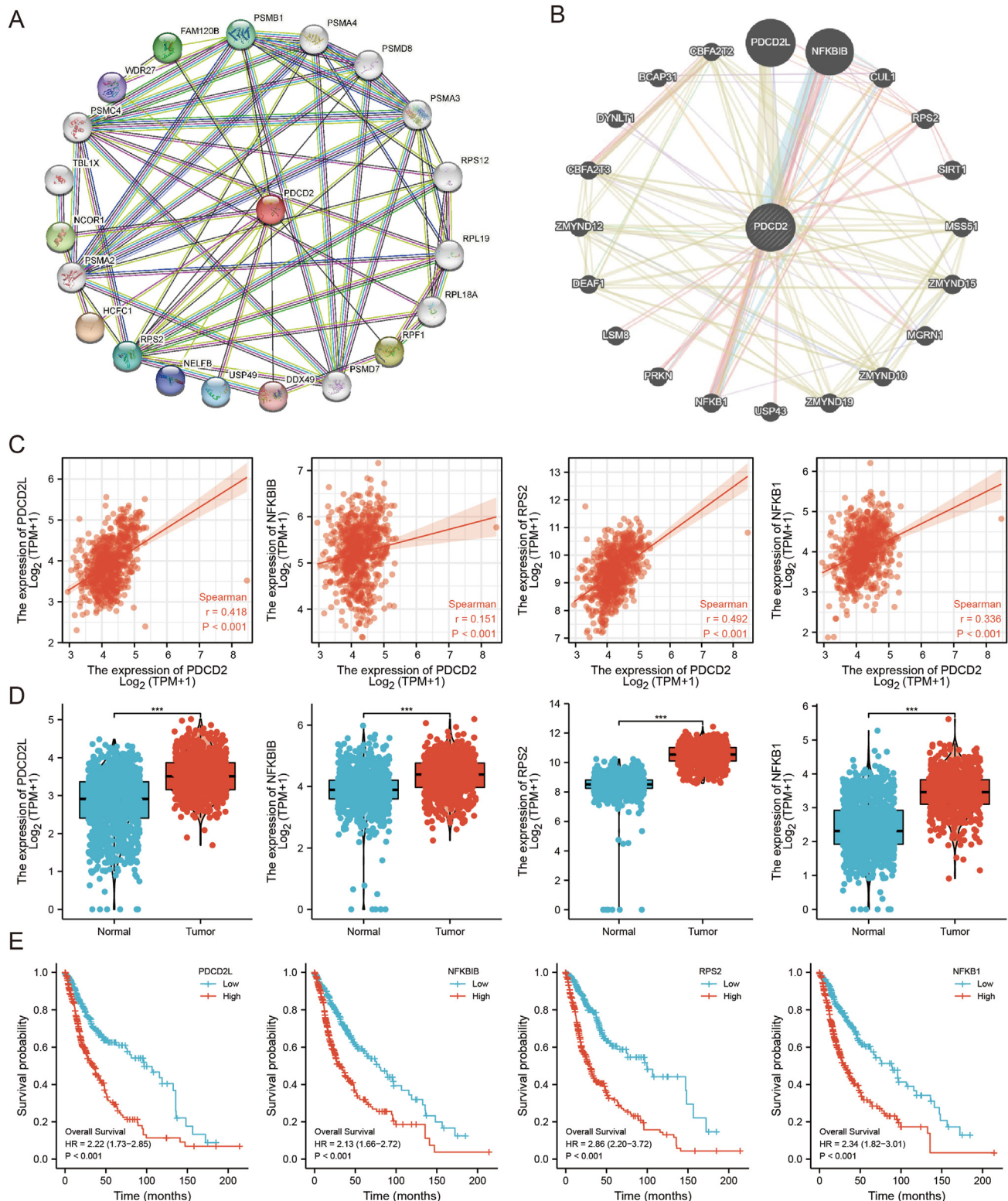
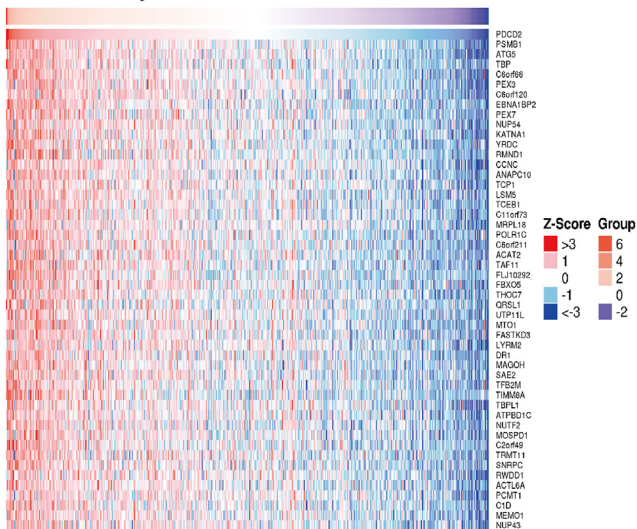
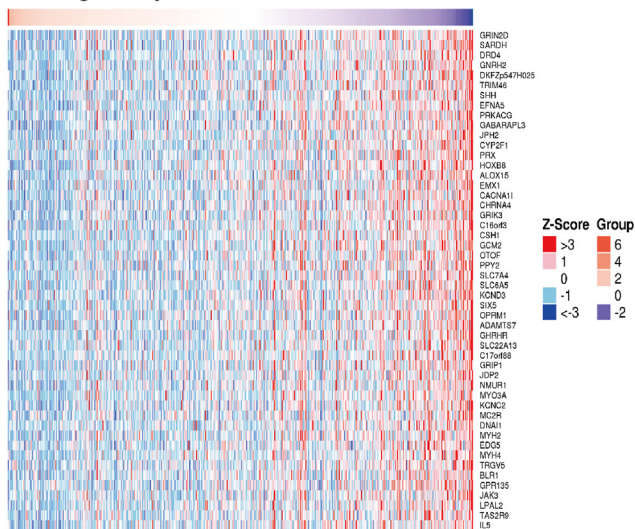


Figure 8 Interaction network of PDCD2. The network of PDCD2 at the protein (A) and gene (B) levels in pan-cancer. Correlation between PDCD2 expression and the expression of PDCD2L, NFKBIB, PRS2, and NFKB1 in GBMLGG (C). (D, E) Expression and prognosis of PDCD2L, NFKBIB, PRS2, and NFKB1 in GBMLGG.

A Positively correlated with PDCD2

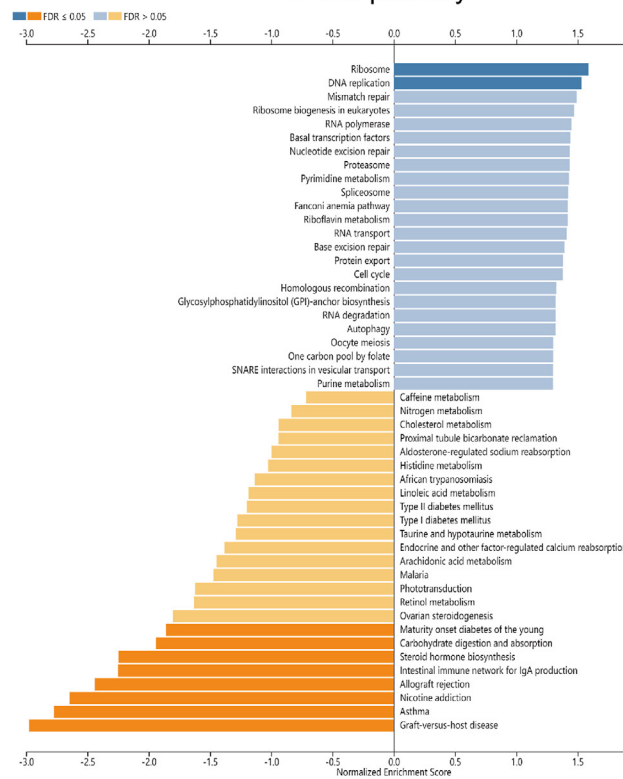


B Negatively correlated with PDCD2



C

KEGG pathway



D

Biology process

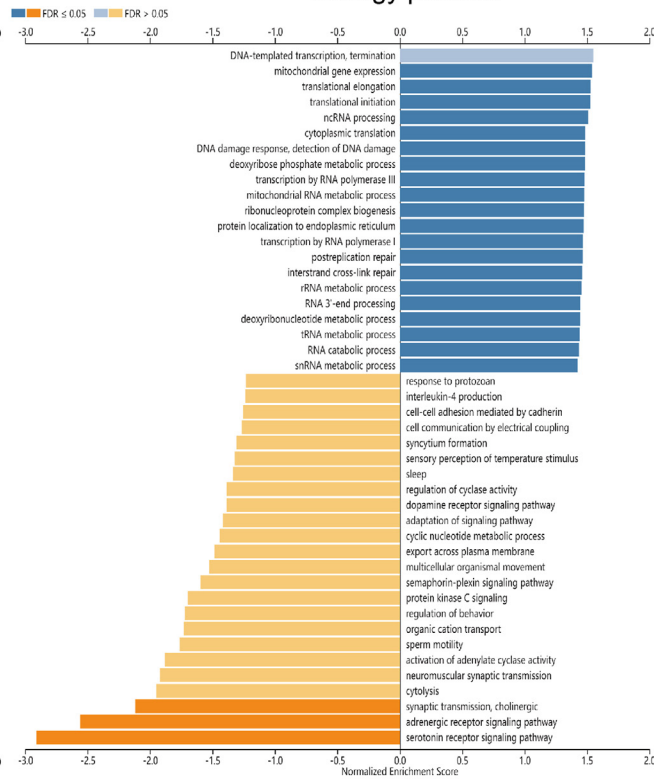


Figure 9 KEGG and GO enrichment analysis for PDCD2. The top 50 genes positively (A) and negatively (B) correlated with PDCD2 are shown in the heat map. (C, D) KEGG pathway (C) and biology process analysis (D) of PDCD2.

patients with many clinical features, including 1p/19q co-deletion status, gender (both female and male), race, age, and histological type, those with high PDCD2 expression have a poor prognosis (Fig. 6A–G). To investigate whether PDCD2 could act as a biomarker in GBMLGG, the ROC curve analysis was performed, and the results indicated that PDCD2 could be used as a high-sensitivity and specificity biomarker to diagnose GBMLGG (Fig. S2A–D). Univariate and multivariate Cox regression analysis revealed that WHO

grade, IDH status, primary therapy outcome, age, histological type, and PDCD2 expression were significantly associated with OS (Table 1).

The TCGA-GBMLGG cohort was also used to construct a nomogram to predict OS, disease-free survival (DFS), and progression-free survival (PFS). In the nomogram, pathological stage and PDCD2 expression acted as prognostic factors (Fig. 7A–C). The calibration curves indicated that the nomogram could reliably predict 1-, 3-, and 5-year OS,

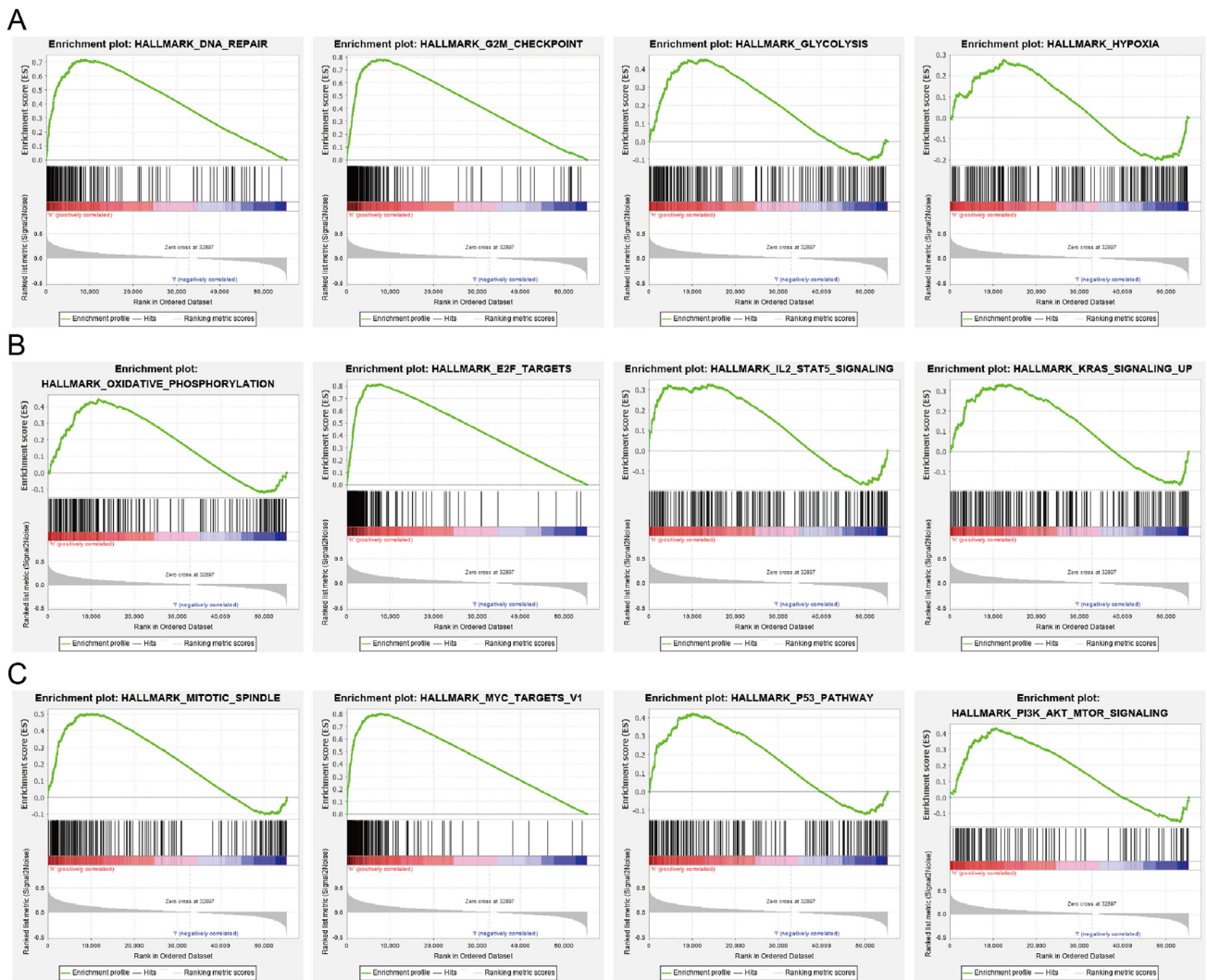


Figure 10 GSEA enrichment PDCD2-related signaling pathway in GBMLGG.

DFS, and PFS in GBMLGG (Fig. 7D–F). In summary, the nomogram has a good ability to predict the GBMLGG patients' prognosis.

Interaction network of PDCD2 in GBMLGG

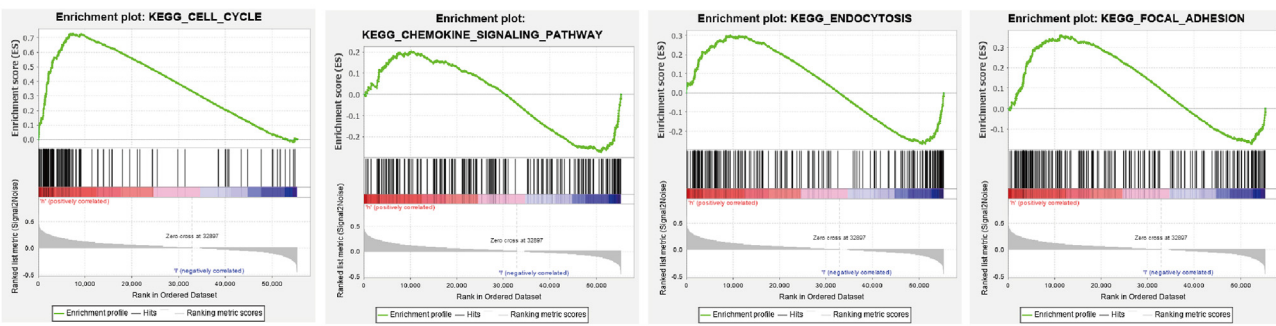
The network of PDCD2 at the protein and gene levels in pan-cancer was shown in Figure 8A and 8B. After examined the association between these genes and PDCD2 in GBMLGG, we discovered a noteworthy positive correlation between PDCD2 and the expression of PDCD2L, NFKB1, PRS2, and NFKB1 as depicted in Figure 9C. Additional analysis revealed that GBMLGG exhibited significant up-regulation of the four genes, which was associated with a poorer prognosis among patients (Fig. 8D, E).

Function analysis of PDCD2 in GBMLGG

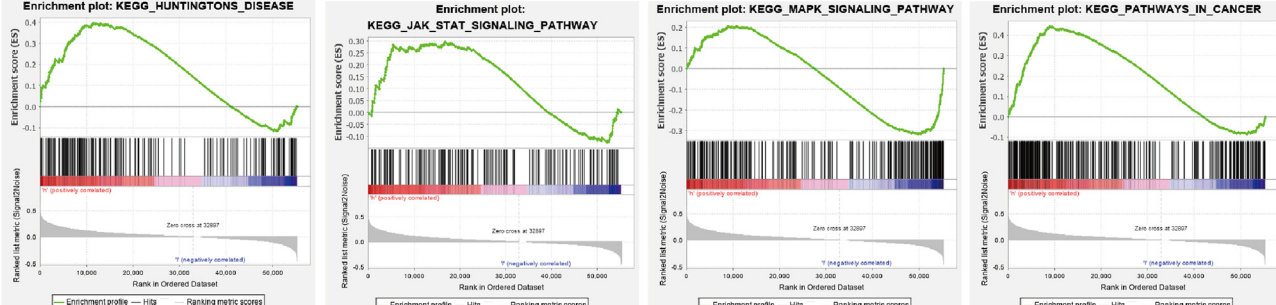
Using Linked-omics, we performed a correlation analysis of PDCD2 in GBMLGG to further determine its possible function. A heat map was constructed to illustrate the

genes whose expression was more positively and negatively correlated with that of PDCD2 (Fig. 9A, B). KEGG pathway analysis showed the enrichment in the ribosome, DNA replication, asthma, nicotine addiction, allograft rejection, the intestinal immune network for IgA production, carbohydrate digestion and absorption, and maturity-onset diabetes of the young (Fig. 9C). GO annotation revealed these genes' participation in mitochondrial elongation, translational initiation, ncRNA processing, cytoplasmic translation, DNA damage response, detection of DNA damage, deoxyribose phosphate metabolic process, transcription by RNA polymerase III, mitochondrial RNA metabolic process, ribonucleoprotein complex biogenesis, protein localization to the endoplasmic reticulum, transcription by RNA polymerase I, post replication repair, interstrand cross-link repair, rRNA metabolic process, RNA 3'-end processing, deoxyribonucleotide metabolic process, RNA catabolic process, snRNA metabolic process, serotonin receptor signaling pathway, adrenergic receptor signaling pathway, and synaptic transmission (Fig. 9D).

A



B



C

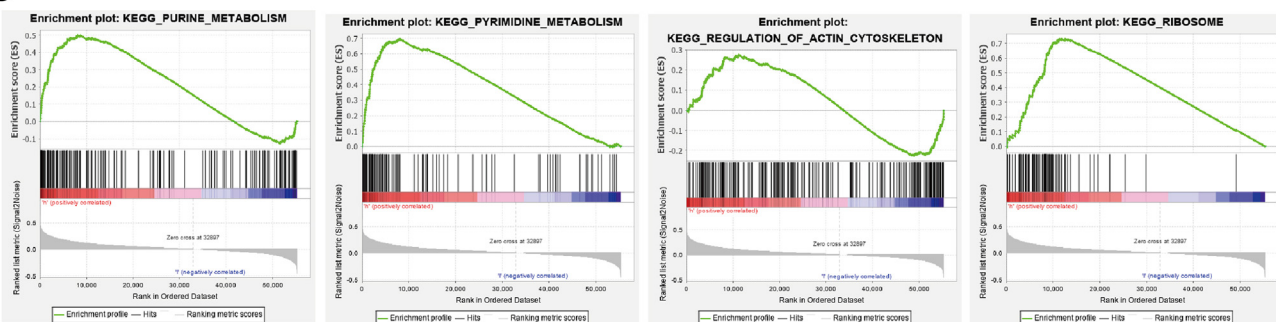


Figure 11 KEGG enrichment PDCD2-related signaling pathway in GBMLGG.

GSEA identification of PDCD2-associated signaling pathways in GBMLGG

PDCD2 participates mainly in the biological processes associated with GBMLGG, according to the GSEA-enriched analysis we performed. Hallmark characteristic enriched results indicated that PDCD2 was enriched primarily in the regulation of DNA repair, G2M checkpoint, P53 pathway, glycolysis, hypoxia, oxidative phosphorylation, E2F targets, IL2 stat5 signaling, MYC targets, KRAS signaling, mitotic spindle, and PI3K/AKT/mTOR signaling (Fig. 10). In addition, KEGG enriched results showed that PDCD2 was mainly involved in cell cycle, pyrimidine metabolism, purine metabolism, endocytosis, focal adhesion, Huntington's disease, JAK/STAT signaling pathway, MAPK signaling pathway, chemokine signaling pathway, pathways in cancer, regulation of actin cytoskeleton, and ribosome (Fig. 11A–C).

PDCD2 promotes GBMLGG cell migration, invasion, and xenograft tumor growth

First, we selected GBMLGG cell lines U251 and U87 with a high malignant degree. The next step was to design and synthesize two siRNAs that specifically targeted PDCD2. U251 and U87 cell lines were transfected with siRNA, and qPCR and Western blotting were conducted to assess knockdown efficiency. Both siRNAs were significantly effective in reducing PDCD2 expression (Fig. 12A, B). Using the CCK-8 assay, we also found that knocking down PDCD2 significantly inhibited the viability of GBMLGG cells (Fig. 12C). Colony formation was significantly inhibited in colonies formed by U251 and U87 cells when PDCD2 was knocked down (Fig. 12D). We also examined the impact of PDCD2 on the migration and invasion of GBMLGG cells using transwell experiments. The results indicated that the suppression of PDCD2 greatly decreased migration and invasion (Fig. 12E, F). Further, we examined

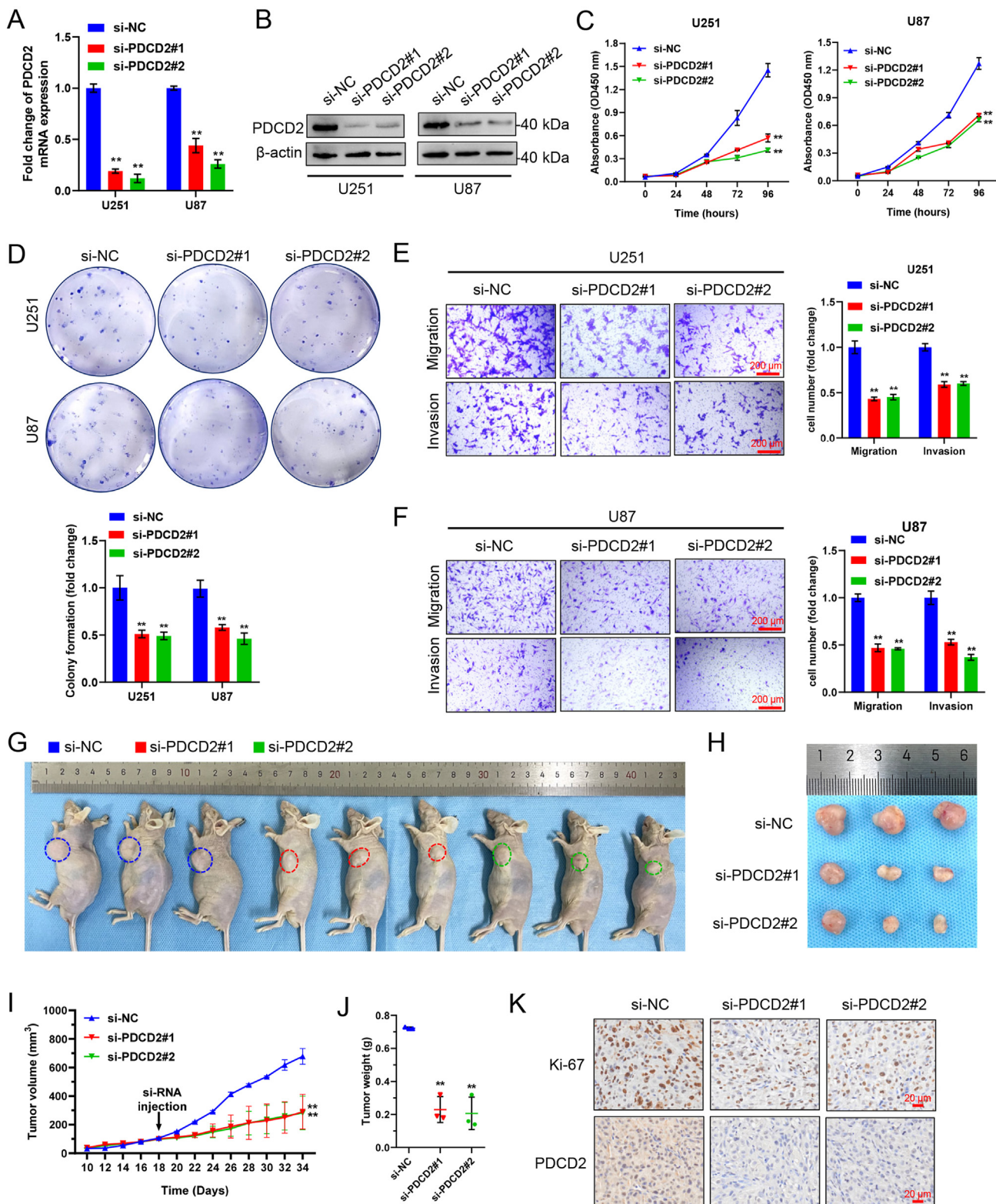


Figure 12 PDCD2 promotes GBMLGG progression. **(A, B)** To determine the levels of PDCD2 expression in U251 and U87 cells transfected with siRNA targeting PDCD2, qPCR and Western blotting were employed. **(C)** Cell growth ability was assessed using CCK8 assays at the specified time intervals in U251 and U87 cells transfected with PDCD2 siRNAs. **(D)** PDCD2 knockdown inhibited colony formation of both U251 and U87 cells. **(E, F)** The migration and invasion of U251 and U87 cells were found to be inhibited by PDCD2 knockdown, as demonstrated by the transwell migration and invasion assays (scale bars = 200 μ m). U87 cells were injected subcutaneously into nude mice to establish a xenograft model. Following the development of the tumor, intertumoral injection of si-PDCD2 or NC was performed ($n = 3$ /group). **(G–I)** Representative pictures and tumor growth chart at 16 days post-injection of si-

the impact of PDCD2 on GBMLGG in an *in vivo* setting by utilizing a xenograft tumor model. Tumors were injected with NC or PDCD2 siRNA every other day, starting from Day 18, and the mice were euthanized on Day 34. The tumor growth curve indicated that the growth rate of xenograft tumors created by U87 cells with reduced PDCD2 levels was noticeably decreased in comparison to the NC (Fig. 12G–I). The xenograft tumors that received si-PDCD2 had a lower weight compared with those in the NC group (Fig. 12J). In si-PDCD2 injected xenograft tumors, IHC staining indicated a reduction in the expression of Ki67 and PDCD2 compared with the NC group (Fig. 12K). These findings indicate that PDCD2 might be responsible for GBMLGG's oncogenic effects.

Discussion

Comparing heterogeneity between various tumors through pan-cancer analysis is essential for the discovery of new cancer biomarkers and therapeutic targets.³² The involvement of PDCD2 in the development of lymphomas in human B and T cells has been shown.¹⁰ PDCD2 can also predict the occurrence of leukemia.⁸ At present, there have been no investigations conducted to determine if PDCD2 is linked to overall cancer prognosis.

During this study, it was observed that PDCD2 expression levels were notably elevated in various forms of malignancies. Furthermore, a strong association was identified between PDCD2 expression and unfavorable OS rates in cases of ACC, GBMLGG, LIHC, and SARC. Similarly, a negative correlation was found between PDCD2 expression and DSS rates in ACC, GBMLGG, and UCEC, as well as poor PFI rates in ACC, GBMLGG, HNSC, LIHC, OV, and UCEC. ROC curve analysis indicates that PDCD2 could serve as a highly specific and sensitive biomarker for the diagnosis of different types of cancers.

In addition, our team verified the correlation between PDCD2 and genetic mutation. The highest frequency of PDCD2 alterations (>6%) was observed in ocular melanoma. Additionally, we verified that the rates of modification were 3.3%, 3.25%, and 2.73% in ocular melanoma, ACC, and ovarian epithelial tumors, respectively.

Glioma is a common malignant tumor of the central nervous system. This tumor type has the characteristics of rapid growth and poor prognosis. In addition, the clinical treatment effect is not satisfactory.^{1,33} In the TCGA GBMLGG cohort, decreased levels of PDCD2 expression and pathological stage were significantly associated with better OS, DSS, and PFS outcomes. Based on the calibration curves, the nomogram could reliably predict 1-, 3-, and 5-year OS in GBMLGG. KEGG and GO enrichment, GSEA analysis, and gene–gene interaction analysis were all employed to investigate PDCD2's role in GBMLGG. It appears that PDCD2 plays an important role in GBMLGG, as indicated by all these results. Moreover, we found that

PDCD2 could significantly promote the proliferation, migration, and invasion of GBMLGG cells.

Now, we have a better understanding of how PDCD2 plays a role in pan-cancer, but there are still some inconsistencies. Despite having explored the relationship between PDCD2 and prognosis in pan-cancer, PDCD2 function has only been confirmed in GBMLGG, but further *in vivo* and *in vitro* studies are needed to elucidate its molecular mechanism in cancer development.

Conclusions

To sum up, our findings indicate that PDCD2 may play a role in pan-cancer as well as in its prognosis and diagnosis. Decreased PDCD2 expression level was directly related to better survival outcomes of GBMLGG. PDCD2 also could inhibit GBMLGG cell proliferation, migration, and invasion. As a molecular predictor of cancer prognosis, PDCD2 can be used clinically to detect GBMLGG.

Ethics declaration

This study was authorized by the Institutional Ethics Committees of the First Affiliated Hospital of Chongqing Medical University (approval notice: IACUC-CQMU-2023-0172) and abided by the Declaration of Helsinki.

Author contributions

TX supervised the manuscript and designed this study. FD, YY, and JH designed this study, performed related assays, and analyzed the data. FD, XC, XZ, LZ, RT, and YZ contributed study materials. All authors read and approved the final version of the manuscript.

Conflict of interests

The authors declare no competing interests.

Funding

This study was supported by the National Natural Science Foundation of China (No. 82172619), the Natural Science Foundation of Chongqing, China (No. CSTC2021jscx-gksb-N0023), and the Fundamental Research Funds for the Central Universities in China (No. 2022CDJYGRH-002).

Appendix A. Supplementary data

Supplementary data to this article can be found online at <https://doi.org/10.1016/j.gendis.2023.101106>.

PDCD2 or NC in GBMLGG xenograft model. (J) The weight of the xenograft tumor was measured and graphed 16 days after the injection. (K) IHC staining was used to examine the alterations in the levels of PDCD2 and Ki-67 in xenograft tumors. Representative images are shown (scale bars = 20 μm). The data were presented as mean ± standard deviation of three independent experiments. *P < 0.05, **P < 0.01, ***P < 0.001.

References

1. Sung H, Ferlay J, Siegel RL, et al. Global cancer statistics 2020: GLOBOCAN estimates of incidence and mortality worldwide for 36 cancers in 185 countries. *CA Cancer J Clin.* 2021;71(3):209–249.
2. Hanahan D. Hallmarks of cancer: new dimensions. *Cancer Discov.* 2022;12(1):31–46.
3. Cao J, Yan Q. Cancer epigenetics, tumor immunity, and immunotherapy. *Trends Cancer.* 2020;6(7):580–592.
4. Owens GP, Hahn WE, Cohen JJ. Identification of mRNAs associated with programmed cell death in immature thymocytes. *Mol Cell Biol.* 1991;11(8):4177–4188.
5. Minakhina S, Druzhinina M, Steward R. Zfrp8, the *Drosophila* ortholog of PDCD2, functions in lymph gland development and controls cell proliferation. *Development.* 2007;134(13):2387–2396.
6. Mu W, Munroe RJ, Barker AK, Schimenti JC. PDCD2 is essential for inner cell mass development and embryonic stem cell maintenance. *Dev Biol.* 2010;347(2):279–288.
7. Landry-Voyer AM, Bergeron D, Yague-Sanz C, Baker B, Bachand F. PDCD2 functions as an evolutionarily conserved chaperone dedicated for the 40S ribosomal protein uS5 (RPS2). *Nucleic Acids Res.* 2020;48(22):12900–12916.
8. Barboza N, Minakhina S, Medina DJ, et al. PDCD2 functions in cancer cell proliferation and predicts relapsed leukemia. *Cancer Biol Ther.* 2013;14(6):546–555.
9. Baron BW, Hyjek E, Gladstone B, Thirman MJ, Baron JM. PDCD2, a protein whose expression is repressed by BCL6, induces apoptosis in human cells by activation of the caspase cascade. *Blood Cells Mol Dis.* 2010;45(2):169–175.
10. Baron BW, Zeleznik-Le N, Baron MJ, et al. Repression of the PDCD2 gene by BCL6 and the implications for the pathogenesis of human B and T cell lymphomas. *Proc Natl Acad Sci U S A.* 2007;104(18):7449–7454.
11. Wang W, Song XW, Bu XM, Zhang N, Zhao CH. PDCD2 and NCoR1 as putative tumor suppressors in gastric gastrointestinal stromal tumors. *Cell Oncol.* 2016;39(2):129–137.
12. Liu H, Wang M, Liang N, Guan L. PDCD2 sensitizes HepG2 cells to sorafenib by suppressing epithelial-mesenchymal transition. *Mol Med Rep.* 2019;19(3):2173–2179.
13. Zhang J, Wei W, Jin HC, Ying RC, Zhu AK, Zhang FJ. Programmed cell death 2 protein induces gastric cancer cell growth arrest at the early S phase of the cell cycle and apoptosis in a p53-dependent manner. *Oncol Rep.* 2015;33(1):103–110.
14. Goldman MJ, Craft B, Hastie M, et al. Visualizing and interpreting cancer genomics data via the Xena platform. *Nat Biotechnol.* 2020;38(6):675–678.
15. Zhao Z, Zhang KN, Wang Q, et al. Chinese glioma genome atlas (CGGA): a comprehensive resource with functional genomic data from Chinese glioma patients. *Genom Proteom Bioinform.* 2021;19(1):1–12.
16. Chandrashekhar DS, Karthikeyan SK, Korla PK, et al. UALCAN: an update to the integrated cancer data analysis platform. *Neoplasia.* 2022;25:18–27.
17. Chandrashekhar DS, Bashel B, Balasubramanya SAH, et al. UALCAN: a portal for facilitating tumor subgroup gene expression and survival analyses. *Neoplasia.* 2017;19(8):649–658.
18. Tang Z, Li C, Kang B, Gao G, Li C, Zhang Z. GEPIA: a web server for cancer and normal gene expression profiling and interactive analyses. *Nucleic Acids Res.* 2017;45(W1):W98–W102.
19. Mizuno H, Kitada K, Nakai Sarai A. PrognoScan: a new database for meta-analysis of the prognostic value of genes. *BMC Med Genom.* 2009;2:18.
20. Cerami E, Gao J, Dogrusoz U, et al. The cBio cancer genomics portal: an open platform for exploring multidimensional cancer genomics data. *Cancer Discov.* 2012;2(5):401–404.
21. Subramanian A, Tamayo P, Mootha VK, et al. Gene set enrichment analysis: a knowledge-based approach for interpreting genome-wide expression profiles. *Proc Natl Acad Sci U S A.* 2005;102(43):15545–15550.
22. Liberzon A, Subramanian A, Pinchback R, Thorvaldsdóttir H, Tamayo P, Mesirov JP. Molecular signatures database (MSigDB) 3.0. *Bioinformatics.* 2011;27(12):1739–1740.
23. Warde-Farley D, Donaldson SL, Comes O, et al. The GeneMANIA prediction server: biological network integration for gene prioritization and predicting gene function. *Nucleic Acids Res.* 2010;38(suppl_2):W214–W220.
24. Szklarczyk D, Gable AL, Lyon D, et al. STRING v11: protein-protein association networks with increased coverage, supporting functional discovery in genome-wide experimental datasets. *Nucleic Acids Res.* 2019;47(D1):D607–D613.
25. Zhang Y, Fan J, Fan Y, et al. The new 6q27 tumor suppressor DACT2, frequently silenced by CpG methylation, sensitizes nasopharyngeal cancer cells to paclitaxel and 5-FU toxicity via β-catenin/Cdc25c signaling and G2/M arrest. *Clin Epigenet.* 2018;10(1):26.
26. Xiang T, Tang J, Li L, et al. Tumor suppressive BTB/POZ zinc-finger protein ZBTB28 inhibits oncogenic BCL6/ZBTB27 signaling to maintain p53 transcription in multiple carcinogenesis. *Theranostics.* 2019;9(26):8182–8195.
27. Wu Y, Zhang Y, Zheng X, et al. Circular RNA circCORN1C promotes laryngeal squamous cell carcinoma progression by modulating the let-7c-5p/PBX3 axis. *Mol Cancer.* 2020;19(1):99.
28. Li L, Gong Y, Xu K, et al. ZBTB28 induces autophagy by regulation of FIP200 and Bcl-XL facilitating cervical cancer cell apoptosis. *J Exp Clin Cancer Res.* 2021;40(1):150.
29. Gao W, Zhang C, Li W, et al. Promoter methylation-regulated miR-145-5p inhibits laryngeal squamous cell carcinoma progression by targeting FSCN1. *Mol Ther.* 2019;27(2):365–379.
30. Madhavan S, Zenklusen JC, Kotliarov Y, Sahni H, Fine HA, Buetow K. Rembrandt: helping personalized medicine become a reality through integrative translational research. *Mol Cancer Res.* 2009;7(2):157–167.
31. Gravendeel LAM, Kouwenhoven MCM, Gevaert O, et al. Intrinsic gene expression profiles of gliomas are a better predictor of survival than histology. *Cancer Res.* 2009;69(23):9065–9072.
32. Dohmlan AB, Arguijo Mendoza D, Ding S, et al. The cancer microbiome atlas: a pan-cancer comparative analysis to distinguish tissue-resident microbiota from contaminants. *Cell Host Microbe.* 2021;29(2):281–298.e5.
33. Gusyatiner O, Hegi ME. Glioma epigenetics: from subclassification to novel treatment options. *Semin Cancer Biol.* 2018;51:50–58.